Aberystwyth University

Generating long chronologies for lacustrine sediments using luminescence dating

Roberts, Helen M.; Bryant, Charlotte L.; Huws, Dei; Lamb, Henry

Published in:
Quaternary Science Reviews

DOI:
10.1016/j.quascirev.2018.10.037

Publication date:
2018

Citation for published version (APA):
Roberts, H. M., Bryant, C. L., Huws, D., & Lamb, H. (2018). Generating long chronologies for lacustrine sediments using luminescence dating: A 250,000 year record from Lake Tana, Ethiopia. *Quaternary Science Reviews*, *202*, 66-77. https://doi.org/10.1016/j.quascirev.2018.10.037

Document License
CC BY

General rights
Copyright and moral rights for the publications made accessible in the Aberystwyth Research Portal (the Institutional Repository) are retained by the authors and/or other copyright owners and it is a condition of accessing publications that users recognise and abide by the legal requirements associated with these rights.

• Users may download and print one copy of any publication from the Aberystwyth Research Portal for the purpose of private study or research.
• You may not further distribute the material or use it for any profit-making activity or commercial gain
• You may freely distribute the URL identifying the publication in the Aberystwyth Research Portal

Take down policy
If you believe that this document breaches copyright please contact us providing details, and we will remove access to the work immediately and investigate your claim.

tel: +44 1970 62 2400
email: is@aber.ac.uk

Download date: 16. Jun. 2024

Quaternary Science Reviews 202 (2018) 66–77

Contents lists available at ScienceDirect

Quaternary Science Reviews

journal homepage: www.elsevier.com/locate/quascirev

Generating long chronologies for lacustrine sediments using luminescence dating: a 250,000 year record from Lake Tana, Ethiopia

Helen M. Roberts [a,*], Charlotte L. Bryant [b], Dei G. Huws [c], Henry F. Lamb [a]

[a] Department of Geography and Earth Sciences, Aberystwyth University, Aberystwyth, Wales, SY23 3DB, UK
[b] NERC Radiocarbon Facility, Scottish Enterprise Technology Park, Rankine Avenue, East Kilbride, G75 0QF, UK
[c] School of Ocean Sciences, Bangor University, Menai Bridge, Anglesey, LL59 5AB, UK

ARTICLE INFO

Article history:
Received 9 March 2018
Received in revised form
31 October 2018
Accepted 31 October 2018
Available online 17 November 2018

Keywords:
Palaeolimnology
Luminescence dating
Post-IR IRSL signal
Polymineral fine-grains
Lacustrine sediments
Direct dating
OSL
Radiocarbon

ABSTRACT

The lakes of the eastern Africa Rift often contain great thicknesses of sediment that may provide continuous records of environmental change over decadal to million-year timescales. However interpretation of these changes is greatly compromised without a reliable chronology. Luminescence dating has not been used extensively in lacustrine settings; instead previous studies have often relied upon radiocarbon dating, using extrapolation beyond the upper limit of that technique, and employing opportunistic sampling of tephra and palaeomagnetic signatures where possible. This study from Lake Tana, Ethiopia, demonstrates that recent advances in luminescence methodology can provide long chronologies for lake sediments that are not dependent on the intermittent presence of dateable material, as is the case for radiocarbon and tephra-based methods. Specifically, this study generates luminescence ages that agree with independent chronology based on radiocarbon dating in the upper part of the core, and extends significantly beyond the range of radiocarbon dating to provide one of the longest independently dated lacustrine sediment records in eastern Africa, thus demonstrating the tremendous potential of luminescence for constructing lacustrine sediment chronologies over 100,000 year timescales.

© 2018 The Authors. Published by Elsevier Ltd. This is an open access article under the CC BY license (http://creativecommons.org/licenses/by/4.0/).

1. Introduction

Lakes can preserve some of the best terrestrial records of environmental change, often providing high-resolution temporally continuous datasets. Lakes on the African continent, and in many other middle and low-latitude settings, offer the opportunity to examine long palaeoenvironmental records, some of which are relevant to the study of human evolution and dispersal, whilst others are derived from climatically-sensitive areas. It is not uncommon for sediment cores of many tens, and even hundreds of metres length, to be retrieved (e.g. Cohen et al., 2016). However, although some of these thick sedimentary deposits reveal detailed fluctuations in palaeoenvironmental proxies, such information is of limited value without a reliable chronology.

Thus far, lake sediment chronologies have been chiefly reliant on radiocarbon dating, which typically restricts the ages generated to the last ~45 ka (e.g. Burnett et al., 2011). However, this time range frequently covers only the upper portion of the sediment record, and the deeper portions are assigned ages by extrapolation (e.g. Burnett et al., 2011). Such an approach assumes a continuous sediment record with no hiatus, and a constant sediment accumulation rate over time. An alternative approach taken to assign ages beyond the limit of radiocarbon dating is to tune one of the palaeoenvironmental proxies to orbital insolation (e.g. Partridge et al., 1997), but this may involve inherently circular reasoning when trying to interpret the proxy record.

A preferable approach is direct dating of the sediments throughout the entire sequence. Luminescence dating can span an extended time range compared to radiocarbon dating (e.g. typically of the order of 10^1–10^5 years), and the technique also offers the advantage of dating the time of deposition of sediments directly using the commonly occurring minerals, quartz and feldspar. Unlike radiocarbon or tephrochronological approaches, luminescence dating is not restricted by the need to find sufficient suitable material in situ, and hence luminescence techniques can be applied at any depth of interest in a sedimentary sequence. However, the application of luminescence dating to lake floor (as opposed to shoreline) deposits has been surprisingly limited, and typically

* Corresponding author.
E-mail address: hmr@aber.ac.uk (H.M. Roberts).

https://doi.org/10.1016/j.quascirev.2018.10.037
0277-3791/© 2018 The Authors. Published by Elsevier Ltd. This is an open access article under the CC BY license (http://creativecommons.org/licenses/by/4.0/).

focussed on mid-high latitudes (e.g. Doran et al., 1999; Vandergoes et al., 2005; Forman et al., 2007; Juschus et al., 2007; Moska et al., 2008; Long et al., 2011), with few studies applying luminescence techniques to African lacustrine sediment sequences (e.g. Scholz et al., 2007; Kadereit et al., 2012; Shanahan et al., 2013 working with lakes Bosumptwi, Malawi, and Tanganyika). Studies of lake sediments have reported mixed success using various different luminescence techniques over the years, which in part echoes the development of the method as a whole. However, recent advances in luminescence methodology and improvements in both the accuracy and precision of luminescence dating, means that these techniques can now make a valuable contribution to the construction of chronologies from lake sediments.

1.1. Recent advances in luminescence dating

Luminescence dating techniques are applied directly to grains of sedimentary quartz and/or feldspar, and they use a time-dependent signal that accumulates over the period since their deposition. The luminescence signal of interest for dating is stimulated in the laboratory by exposure of mineral grains to light (giving an 'optically stimulated luminescence', OSL, signal). In the case of most sediments in the natural environment, the event being dated is the last exposure of the mineral grains to daylight, and therefore the luminescence age relates directly to the time of deposition.

Recent improvements in luminescence dating techniques (e.g. discussed in Roberts, 2008 and Rhodes, 2011) have brought about a step-change in the accuracy, precision, and hence in the confidence of dating using optically stimulated luminescence dating applied to quartz. Comparisons of quartz OSL ages generated using the Single Aliquot Regenerative dose (SAR) measurement protocol (Murray and Wintle, 2000) with independent age control in the range from 10^1 to 10^5 years have demonstrated excellent agreement (e.g. Murray and Olley, 2002; Rittenour, 2008), leading to quartz arguably being the mineral of choice for luminescence dating since 2000. Feldspars have the potential to span a greater age range than quartz, but the biggest single factor preventing the widespread adoption of feldspar for luminescence dating has been the phenomenon of 'anomalous fading'. Anomalous fading (Wintle, 1973) involves the loss of some trapped charge over time (rather than a simple, steady build-up of charge as seen for quartz) and is thought by some authors to be ubiquitous, affecting all feldspars (Huntley and Lamothe, 2001). Where anomalous fading occurs, it results in feldspar ages that are erroneously young. Until recently, the approach adopted to compensate for anomalous fading was to attempt to measure the degree of fading, and correct for this in the final age calculation. However, such measurement can be difficult, and there is no agreed method for either detection of, or correction for, anomalous fading in feldspars. Correction methods have typically only been applied to the linear portion of the feldspar dose response curve, which in many cases means that they can only be applied in a similar dose range to that of quartz; hence any potential advantage of using feldspars to extend the luminescence age range beyond that of quartz is lost. Kars et al. (2008) proposed a method with the potential to correct for anomalous fading beyond this linear region, although this approach has achieved mixed success (e.g. Kars and Wallinga, 2009; Morthekai et al., 2011; Guralnik et al., 2015; King et al., 2018). An infinitely preferable approach would be to avoid the need for such correction altogether.

In more recent years, an alternative approach to dating using feldspars has been proposed, namely to use a signal from feldspars where the degree of anomalous fading is minimal. Thomsen et al. (2008) investigated the fading rates observed for OSL signals from feldspars under different measurement conditions, and found that fading rates were minimised by using an elevated temperature (225 °C) infra-red stimulated luminescence (IRSL) signal obtained following prior IR stimulation at the more standard low temperature (50 °C) hitherto frequently used for dating. This 'post-IR $IRSL_{225}$' signal typically demonstrated fading rates of ~1%/decade, compared to fading rates of 2–3%/decade for the coarse grained feldspars measured using the more conventional $IRSL_{50}$ signal (Thomsen et al., 2008). The use of a luminescence signal from feldspars that minimises fading avoids the need for any complex fading corrections, and therefore potentially extends the effective luminescence age range beyond the current ~100 ka cap (~150 Gy equivalent dose; Chapot et al., 2012) that exists using quartz OSL. Critically, this also means that luminescence dating can be applied to areas where quartz is either not found in sufficient quantities for dating (e.g. due to the nature of the source rock geology) or where the quartz has poor behavioural characteristics (e.g. low natural signal levels, poor sensitivity, no fast signal component).

1.2. The application of luminescence dating to lake sediments

The major advances in luminescence dating within the last decade described above have permitted the application of this family of techniques to an increasingly broad range of depositional environments, beyond the aeolian deposits where luminescence dating of sediments had much of its early focus. In spite of this, there have been surprisingly few studies applying luminescence dating to lake-floor sediments, particularly in Africa. There, OSL dating has been applied chiefly to palaeoshorelines in the form of beach-ridges. Such features have been dated using OSL applied to coarse-grained quartz (e.g. Burrough et al., 2007; Burrough and Thomas, 2008; Armitage et al., 2015), to constrain the nature and timing of lake highstand events. Whilst the nature of these palaeoshoreline records is rather discontinuous (Burrough and Thomas, 2009), and their interpretation can be challenging (e.g. Chase and Meadows, 2007), they can offer insight into past hydrological conditions (Burrough and Thomas, 2009). There is no *a priori* reason, however, why OSL should not be applied to lacustrine sediments; indeed given the long palaeoenvironmental records preserved in lakes and the relatively short timescale covered by radiocarbon dating, there is every reason why OSL *should* be applied to lake-floor sediments.

One reason for the lack of OSL studies applied to lake sediments may be due to the logistical difficulties of deep-drilling, sometimes over very deep water; the relatively limited sample volumes retrieved are therefore very precious. There may also have been a perception among the non-luminescence community that the material collected was inappropriate for luminescence dating because it was collected within transparent core-liners, and/or split and logged in white-light before sampling. However, such material is still suitable for luminescence dating, even if taken in transparent liners, provided that a sub-sample of material that has not been exposed to light can be removed from the interior of the cores. Even material that has undergone XRF scanning can be suitable for luminescence dating if care is taken in sampling (e.g. see Davids et al., 2010).

Other concerns about the suitability of lake-floor sediments for luminescence dating may have been associated with estimating the past water content, which plays an important role in the assessment of the dose rate (Equation (1)) and therefore impacts upon the luminescence age calculated (e.g. for a given sample there is typically ~1% change in age for every 1% change in water content). The water content of the sediments may have changed over time due to desiccation or wetting of the lake (although deeper sediments are unlikely to have been affected by such events when the average water content of the sediments over the entire time since deposition is considered), and/or the water content may have changed over time due to sediment compaction. While it is important to consider carefully the likely variation in past water content over time, this task is not necessarily more complex for lake-floor sediments than for some other depositional settings where luminescence dating is used more regularly (e.g. fluvial and glacial deposits).

$$\text{Age (ka)} = \frac{\text{Equivalent dose, De (Gy)}}{\text{Dose rate (Gy/ka)}} \quad (1)$$

Additionally, incomplete removal (or 'bleaching') of the pre-existing luminescence signal during transport and deposition has been a concern for lacustrine sediments, because transport or deposition processes commonly involve water. Attenuation of light through the water column reduces the efficacy of bleaching, thus increasing the length of time of exposure that is needed to reset the luminescence signal. The degree of bleaching will vary according to local conditions at a given site, but will be influenced by such factors as the depth and turbidity of the water column, transport distances and processes, etc. Critically, if incomplete bleaching occurs, it would lead to an overestimation of the time elapsed since deposition. In some environments, including some lacustrine settings, an assessment of the degree of bleaching prior to deposition can potentially be made using coarse, sand-sized grains, by examining small numbers of grains for each of a suite of sub-samples ('aliquots') of material, or even examining single-grains, if the signal is sufficiently bright. These measurements of many aliquots reveal the range of equivalent dose (D_e) values (Equation (1)) for the sample, from which the degree of homogeneity of bleaching prior to deposition can potentially be inferred (e.g. see review by Duller, 2008). However, lacustrine sediments are often fine-silt sized, leading to large numbers of grains on each aliquot. This gives rise to averaging of the luminescence signals across aliquots and hence masks variability in the degree of bleaching prior to deposition. However, following the advances in luminescence dating outlined in section 1.1, there are now a number of luminescence signals that can be used for dating, and these have different sensitivities to bleaching in daylight (e.g. Colarossi et al., 2015); comparison of these different luminescence signals obtained from the same sample can offer some insight into the likely efficacy of bleaching prior to deposition (e.g. as demonstrated by Buylaert et al., 2013, for Laguna Potrok Aike, Argentina).

In summary, the application of OSL techniques to lake sediments is now extremely timely, given recent methodological advances in dating precision (from the use of single aliquot methods) and accuracy (using sensitivity-corrected methods for quartz, and methods to minimise anomalous fading of feldspar signals), coupled with the development of multiple luminescence chronometers, and a suite of quality control checks developed to assess the luminescence data generated (e.g. summarised in Roberts (2008) for quartz; see also Buylaert et al., 2012; Roberts, 2012; Li et al., 2014). This paper demonstrates the contribution that can be made by luminescence dating of long sequences of lacustrine sediments, using an example from Lake Tana, Ethiopia. Optically stimulated luminescence (OSL) techniques were applied to a 90 m sediment core to provide one of the longest, independently dated lacustrine chronologies from eastern Africa.

2. Study site

Lake Tana is located in the Ethiopian highlands, at 12°N, 37°15′E and 1830 m altitude (Fig. 1). The lake has a surface area of 3156 km^2, but mean and maximum water depths of only 9 and 14 m respectively (Kebede et al., 2006). Lake Tana is the largest lake in Ethiopia, the third largest in the Nile basin, and is the source of the Blue Nile. The Blue Nile catchment was a vital source of water and nutrient-rich sediments to ancient Egyptian agriculture, and it remains of critical importance to modern-day Egypt and Sudan (Vijverberg et al., 2009).

The Lake Tana basin spans several degrees of latitude and is situated in a climatically sensitive region, being affected by seasonal movement of the Intertropical Convergence Zone (ITCZ), which governs the pattern of rainfall to the African continent (Fig. 1). In the boreal summer months, the ITCZ is located north of Lake Tana, with 70% of the 1410 mm average annual rainfall falling in July and August; whilst from October to May the ITCZ migrates southwards bringing dry conditions to the region (Lamb et al., 2007; Nicholson, 2017).

The geology of the area is principally basaltic rocks (Abate et al., 1998) with no natural source of crystalline quartz. This has important implications for the application of luminescence dating techniques to the sediments of Lake Tana; the absence of quartz means that feldspars must be used for dating, and the volcanic nature of the source rocks implies that the use of conventional luminescence signals from these feldspars would likely lead to erroneously young ages due to anomalous fading (Wintle, 1973; Visocekas and Guérin, 2006). For these reasons, it is important to use a measurement protocol for feldspars that minimises the degree of anomalous fading.

3. Materials and methods

A high-resolution single-channel seismic survey of Lake Tana was conducted in September 2004 using a swept-frequency Geo-acoustic Chirp profiler towed behind a 12 m vessel (see Bates et al., 2007 for further details). This survey, and a further survey conducted in November 2006 using a Boomer Seistec system (Lamb et al., 2018, their supplementary information), were used to identify the most appropriate locations from which to retrieve core samples. In 2007, two cores were taken from Lake Tana, ~10 m apart from each other. Core 07TL1 sampled the upper 8.18 m of lake-floor sediment using a Livingstone piston corer, and deep drill core PT07-2 retrieved sediments from 13.14 to 91.80 m depth using a Boart Longyear LY38 drilling rig with a wire-line retrieval system (see Fig. 1 for sample locations and water depths). Overall core recovery was 80% with most of the missing sediments from below 63 m (Lamb et al., 2018).

Cores were held in cold storage (4 °C) before being split and examined in white light, prior to sampling for luminescence dating under subdued red-lighting conditions to preserve the signal used for dating. Fifteen samples were taken for OSL dating, spanning the full ~90 m of the core, taking care to sample away from any obvious change in stratigraphic unit; 14 of these samples were taken in the upper ~60 m to provide a detailed chronology for the region of the core with the best core recovery, and an additional sample was taken to constrain the age of the base of the core. The light-exposed outer portion of the sediment sample was used to assess the uranium (U), thorium (Th) and potassium (K) concentrations contributing to the dose rate (Gy/ka), shown in Table 2; this was achieved by grinding samples to a fine powder, fusing with lithium metaborate, after which K_2O content was determined using ICP-OES, and U and Th concentrations were measured by ICP-MS. The dose rate (Table 2) was calculated using the conversion factors of Adamiec and Aitken (1998), and an assumed a-value of 0.08 was used (based on Rees-Jones, 1995). The organic content of the sediments was low throughout the core, with an average value of 7.4 ± 1.5% (n = 645; maximum value of 18.6%; minimum value of 3.4%), and hence it is not necessary to consider dose rate attenuation due to organic matter (Divigalpitiya, 1982). Water content is shown in Table 2 as the % of dry mass of sediment, and was

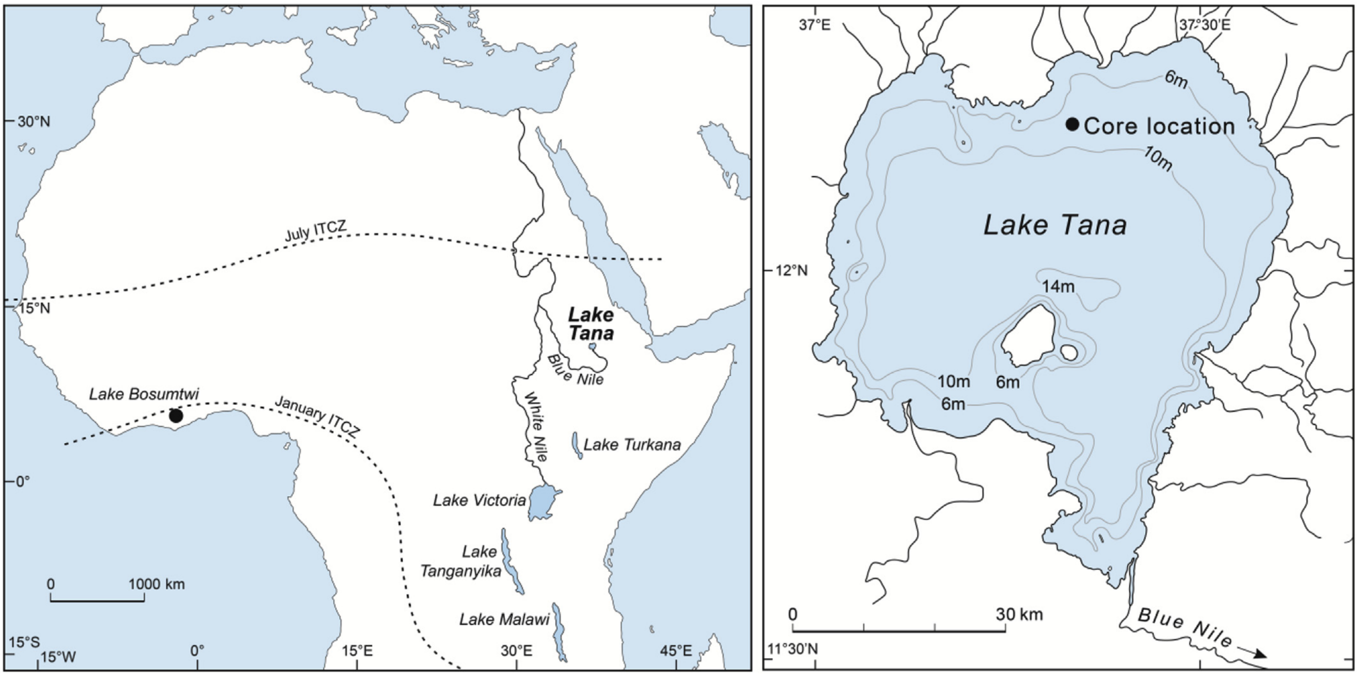

Fig. 1. The location of Lake Tana, NW Ethiopia, showing lake bathymetry and the position of the Intertropical Convergence Zone (ITCZ). The location of the cores used in this study is also shown.

Table 1
Single Aliquot Regenerative dose (SAR) sequence of measurements used in this study to obtain the Post-IR $IRSL_{225}$ signal for dating sediments from Lake Tana.

Step no.	Treatment
1	Natural or Regenerative dose
2	Preheat (250 °C/60s)
3	$IRSL_{50}$ (100s IR stimulation @ 50 °C)
4	Post-IR $IRSL_{225}$ (100s IR stimulation @ 225 °C): L_x
5	Test dose
6	Preheat (250 °C/60s)
7	$IRSL_{50}$ (100s IR stimulation @ 50 °C)
8	Post-IR $IRSL_{225}$ (100s IR stimulation @ 225 °C): T_x

calculated as the mean of the measured water content values (determined every 8 cm depth) for sediments spanning ± 30 cm of the sample taken for luminescence dating. Care was taken to preserve the moisture content of the core following splitting, through cold storage and double-wrapping of the core in thick film, as is common practice in many palaeoenvironmental studies. The dose rate contribution from cosmic rays was calculated according to Prescott and Hutton (1994) using a water depth of 12.5 m overlying the sediment depth down-core, and assigning a dose rate uncertainty of 10%. The maximum depth for which the cosmic dose rate was calculated was 29 m; below this depth the data generated are likely to become increasingly unreliable (Prescott and Hutton, 1994; Grün, 2009). Sensitivity analysis of the effect of changing sample depth over time (conducted using a fixed water depth of 12.5 m, and comparing the dose rate calculated for the deepest sample, both at its present depth and also at the current depth of the uppermost sample in the study) showed that even the greatest change in cosmic dose rate had less than 5% effect on the overall dose rate.

The Lake Tana sediments are chiefly comprised of clay and fine-silt sized material. Such clay-rich sediments can pose problems when preparing fine-grains for luminescence dating, with clay particles flocculating to form larger aggregates, and also clay particles settling over time to form an impermeable barrier between the sediments and the reagents, thereby increasing the time needed to complete the chemical treatments. For these reasons, the sediments in this study were washed repeatedly with a 5% solution of sodium pyrophosphate ($Na_4P_2O_7$) to de-flocculate the clays and also to remove a significant proportion of the clay particles prior to further processing. Polymineral fine grains (i.e. mixed mineralogy grains of 4–11 μm diameter) were then prepared for luminescence dating using standard preparation procedures for small sediment volumes; treatment with 10% v.v. dilution of hydrochloric acid to remove carbonates, followed by 20 vols hydrogen peroxide to remove organics, and finally isolation of the 4–11 μm fraction by Stokes' Law Settling using acetone. As stated, the geology of the catchment does not contain any significant source of quartz, but to investigate whether the lake-floor sediments contained any significant quantity of far-travelled quartz, an attempt was made to isolate pure fine-grained quartz using hydrofluorosilicic acid (H_2SiF_6), but insufficient material for dating was recovered from this acid-etch treatment. From an initial sediment mass of ~40 g, after the preparation described above between 0.1 and 3% by mass was recovered as polymineral fine-grains (4–11 μm). Aliquots of polymineral sample material were prepared for dating by dispensing 1 mg of 4–11 μm diameter material suspended in acetone onto each 9.8 mm diameter aluminium disc.

Measurements of equivalent dose were made using a number of automated Risø TL/OSL readers equipped with $^{90}Sr/^{90}Y$ beta sources delivering a dose to fine-grains of 4.42–5.34 Gy/min. Stimulation was at 870 nm using infra-red (IR) light-emitting diodes, and signals were detected using a combination of Schott BG39, GG-400, and Corning 7–59 filters in front of the photomultiplier tube. Measurements were made using a post-IR IRSL single aliquot regenerative dose (SAR) procedure proposed by Thomsen et al. (2008); a preheat of 250 °C held for 60s was used after

Table 2
Equivalent dose, dose rate, and post-IR IRSL$_{225}$ luminescence ages for polymineral 4–11 μm diameter grains prepared from Lake Tana, Ethiopia.

ALRL[a] Sample No.	Core Number	Stratigraphic depth (m)	Equivalent Dose, D_e (Gy)[b]	No. aliquots used for D_e	Water content[c]	Bulk K (%)[d]	Bulk U (ppm)[d]	Bulk Th (ppm)[d]	Cosmic (Gy/ka)[e]	Total dose rate (Gy/ka)[f]	pIRIRSL$_{225}$ Age (ka)[g]
134/1	07TL1-3	2.86 ± 0.03	2.92 ± 0.19	24	280 ± 28	0.80 ± 0.04	1.62 ± 0.08	7.08 ± 0.35	0.084 ± 0.008	0.68 ± 0.05	4.28 ± 0.43
134/2	07TL1-5	4.22 ± 0.03	5.15 ± 0.20	22	240 ± 24	0.79 ± 0.04	2.21 ± 0.11	9.31 ± 0.47	0.076 ± 0.008	0.90 ± 0.07	5.75 ± 0.51
134/3	07TL1-8	7.55 ± 0.03	7.65 ± 0.25	22	240 ± 24	0.81 ± 0.04	1.79 ± 0.09	8.21 ± 0.41	0.060 ± 0.006	0.79 ± 0.06	9.66 ± 0.81
134/4	PT07-2/5a	14.52 ± 0.03	69.05 ± 1.77	22	50 ± 5	0.96 ± 0.05	1.49 ± 0.07	7.83 ± 0.39	0.040 ± 0.004	1.73 ± 0.12	39.9 ± 2.9
134/5	PT07-2/5b	15.52 ± 0.03	66.29 ± 1.70	12	50 ± 5	1.02 ± 0.05	1.42 ± 0.07	8.40 ± 0.42	0.038 ± 0.004	1.79 ± 0.12	37.0 ± 2.7
134/6	PT07-2/6a	17.52 ± 0.03	83.76 ± 2.26	22	50 ± 5	0.81 ± 0.04	1.61 ± 0.08	6.68 ± 0.33	0.034 ± 0.003	1.57 ± 0.11	53.3 ± 4.1
134/7	PT07-2/8a	23.44 ± 0.03	101.14 ± 2.60	22	50 ± 5	0.96 ± 0.05	2.10 ± 0.11	6.14 ± 0.31	0.026 ± 0.003	1.76 ± 0.12	57.5 ± 4.3
134/8	PT07-2/8c	25.44 ± 0.03	85.07 ± 2.02	17	45 ± 5	0.65 ± 0.03	1.46 ± 0.07	6.87 ± 0.34	0.023 ± 0.002	1.49 ± 0.11	57.3 ± 4.5
134/9	PT07-2/9e	29.06 ± 0.03	76.04 ± 1.56	22	55 ± 6	0.98 ± 0.05	1.95 ± 0.10	6.35 ± 0.32	0.020 ± 0.002	1.68 ± 0.12	45.3 ± 3.3
134/10	PT07-2/11c	34.25 ± 0.03	117.11 ± 2.40	22	60 ± 6	0.81 ± 0.04	1.26 ± 0.06	8.25 ± 0.41	0.000 ± 0.000	1.46 ± 0.11	79.7 ± 6.0
134/11	PT07-2/13b	39.04 ± 0.03	139.41 ± 3.30	22	60 ± 6	0.99 ± 0.05	1.40 ± 0.07	7.67 ± 0.38	0.000 ± 0.000	1.56 ± 0.11	88.9 ± 6.5
134/12	PT07-2/16a	46.99 ± 0.03	151.79 ± 3.75	22	60 ± 6	0.75 ± 0.04	1.74 ± 0.09	7.81 ± 0.39	0.000 ± 0.000	1.55 ± 0.12	97.0 ± 7.9
134/13	PT07-2/19a	54.72 ± 0.03	152.28 ± 4.42	22	40 ± 4	0.92 ± 0.05	1.84 ± 0.09	7.37 ± 0.37	0.000 ± 0.000	1.88 ± 0.14	80.9 ± 6.3
134/14	PT07-2/20b	59.05 ± 0.03	260.72 ± 9.63	15	35 ± 4	0.94 ± 0.05	1.68 ± 0.08	7.66 ± 0.38	0.000 ± 0.000	1.95 ± 0.14	134 ± 11
134/15	PT07-2/31b	89.02 ± 0.03	438.91 ± 10.73	15	35 ± 4	0.54 ± 0.03	1.87 ± 0.09	7.57 ± 0.38	0.000 ± 0.000	1.71 ± 0.14	256 ± 22

[a] Aberystwyth Luminescence Research Laboratory (ALRL) sample number.
[b] The D_e is calculated using the weighted mean, and the error calculated is the standard error on the mean.
[c] Water content is expressed as the % of dry mass of sediment, and calculated as the mean of the measured water content values (determined every 8 cm depth) for sediments spanning ± 30 cm of the sample taken for luminescence dating.
[d] A 5% uncertainty was attributed to each determination based on the reproducibility of analyses over three batches of ICP-MS measurements to determine uranium (U) and thorium (Th) concentrations, and ICP-OES to determine potassium (K) concentrations.
[e] The contribution from cosmic rays was calculated according to Prescott and Hutton (1994), using a water depth of 12.5 m overlying the sediment depth down-core, and assigned an uncertainty of 10%.
[f] Dose rates were calculated using the values of Adamiec and Aitken (1998). An *a*-value of 0.08 ± 0.02 was assumed (Rees-Jones, 1995).
[g] Post-IR IRSL$_{225}$ ages are calculated prior to rounding, expressed as thousands of years before 2010 AD, and shown to three significant figures.

application of regenerative and test doses, followed by 100s IR stimulation at 50 °C, followed by a second 100s IR stimulation but this time at a temperature of 225 °C (Table 1). No high-temperature stimulation (e.g. as used in Buylaert et al., 2009) was used at the end of each measurement cycle because recuperation was less than 1 Gy in absolute terms. Fading tests were conducted according to Auclair et al. (2003), using a modified SAR sequence (regeneration dose ~20 Gy, test dose ~8 Gy) containing a series of delayed and prompt measurements, with delayed measurements taken for each sample over time periods ranging from a few minutes to 1–2 months. Various signal integration limits were explored before adopting the initial 1.2s and the final 20s of each signal to represent the signal and background respectively for dating, in accordance with the "initial signal" integrals used by Thomsen et al. (2008).

4. Results and discussion

4.1. Evaluation of luminescence dating protocol

The measurement sequence used for dating the sediments from Lake Tana is shown in Table 1, and is based upon a method proposed by Thomsen et al. (2008). This sequence uses the 'post IR IRSL$_{225}$' signal for dating (denoted 'L_x' in Table 1). Thomsen et al. (2008) noted that this signal yielded fading rates that were significantly reduced compared to the fading rates of conventional IR signals used for dating (IR measured at 50 °C) for the coarse-grained feldspars in their study. The measurement sequence shown in Table 1 allows both the IRSL$_{50}$ and post-IR IRSL$_{225}$ signals and fading rates to be compared for each polymineral fine-grain aliquot examined in this study (discussed in section 4.3). The suitability of the measurement protocol (Table 1) is demonstrated by all aliquots passing the various screening criteria relating to sufficient signal intensity (i.e. test dose signal uncertainty <10%, and also >3 standard deviations of the background signal), and also having recycling ratios within 10% of unity. A further test on the suitability of any measurement protocol is the ability to accurately assess the magnitude of a known laboratory-given radiation dose; such a 'dose-recovery test' was performed in this study using aliquots prepared from 3 samples. Six aliquots each of Tana samples (prefix 134/) 1, 4 and 9 were freshly prepared, and bleached in a Honlë SOL2 solar simulator for 4 h. Half of the aliquots for each sample were given a laboratory beta dose of ~55 Gy to recover, and the remaining discs were not irradiated but were used for assessment of the residual dose remaining following bleaching; the value of the measured residual dose (1.3 Gy) was subtracted from the dose measured for the discs given a known radiation dose, in order to obtain the dose recovered in response to the given dose of 55 Gy. As sample 134/1 had a post-IR IRSL$_{225}$ D_e that was relatively low (2.92 Gy, i.e. 5.3%) compared to the given dose of 55 Gy, a further dose recovery test was performed using six freshly prepared but unbleached aliquots of sample 134/1, half of which were given a 55 Gy beta dose to recover, and the remaining 3 aliquots were used to assess the 'residual' D_e (in this case, this was the 'natural' D_e value) to subtract in order to assess the dose recovery value for these unbleached aliquots. In all cases, subtracting an appropriate measured residual from either bleached ($n = 9$ aliquots) or unbleached aliquots ($n = 3$) to which a dose of 55 Gy was added, gave a mean ratio of the dose recovered to the dose given which was within 5% of unity (1.02 ± 0.08), indicating that the measurement protocol shown in Table 1 is appropriate for these samples.

4.2. Comparison of IRSL$_{50}$ and post-IR IRSL$_{225}$ signals and D_e values

Fig. 2a shows the raw natural IRSL$_{50}$ and post-IR IRSL$_{225}$ signal decay with stimulation time for a typical aliquot, and the dose response curves for this same aliquot are given in Fig. 2b. The normalised natural signal intensities (L_n/T_n) are seen to be similar for both the IRSL$_{50}$ and post-IR IRSL$_{225}$ signals; however, the normalised dose response curves for the two signals diverge beyond ~100Gy (Fig. 2b). This contrasts with the observations of Buylaert et al. (2009) where the normalised $IRSL_{50}$ and post-IR $IRSL_{225}$ dose response curves were identical, but the normalised natural signals differed. However, the $IRSL_{50}$ signal gives rise to a lower equivalent dose (D_e) value (and hence to a younger final age) than that obtained using the post-IR $IRSL_{225}$ signal (e.g. Fig. 2b). This difference in D_e values has also been observed in other studies (including, and since, Buylaert et al., 2009), and is attributed to post-IR IRSL signals measured at 225 °C being more stable over time (i.e. less prone to anomalous fading) than the IRSL signal measured at 50 °C (Thomsen et al., 2011).

Fig. 3 compares the D_e values obtained for all 15 samples using the $IRSL_{50}$ and post-IR $IRSL_{225}$ signals, demonstrating that the post-IR $IRSL_{225}$ signal gives consistently higher D_e values than would be observed using the hitherto widely used conventional IRSL measurements made at 50 °C. The consistently higher post-IR $IRSL_{225}$ D_e values compared to the $IRSL_{50}$ D_e values are to be expected if, as other studies including Thomsen et al. (2008) have shown, the post-IR $IRSL_{225}$ signals from Lake Tana sediments show lower rates of fading compared to the $IRSL_{50}$ signal. The offset between these two sets of D_e values is in excess of 16% in all cases, ranging to a maximum of 42% (mean ratio $IRSL_{50}$:post-IR $IRSL_{225} = 0.74 \pm 0.07$, $n = 15$ samples, a total of 291 aliquots; Fig. 3). Comparison of the $IRSL_{50}$ and corresponding post-IR $IRSL_{225}$ D_e values obtained for a suite of sediment samples has been proposed by Buylaert et al. (2013) as a means of gaining insight into the degree of bleaching of these luminescence signals prior to deposition. This test of the efficacy of bleaching exploits the fact that the $IRSL_{50}$ signal bleaches more rapidly than post-IR IRSL signals (e.g. Thomsen et al., 2008; Colarossi et al., 2015). In a study of coarse-grained feldspars in lacustrine sediments from Laguna Potrok Aike, through comparison of $IRSL_{50}$ and post-IR IRSL D_e values, Buylaert et al. (2013; their Fig. 7b) identified several samples that may have been incompletely bleached prior to deposition. However, in the case of the fine-silts from Lake Tana, when errors are taken into account there is no significant deviation from the single saturating exponential function fitted to the dataset (Fig. 3). This suggests that all sediments in the present study have been bleached to the same degree prior to deposition; rather than being equally heterogeneously bleached, the simplest explanation is that all samples were fully-bleached at the time of deposition.

4.3. Signal stability – anomalous fading

The offset between the D_e values obtained using the $IRSL_{50}$ and post-IR $IRSL_{225}$ signals (Fig. 3) was anticipated primarily to be due to differences in the stability of these two signals. For this reason, measurements of the degree of anomalous fading were made for the $IRSL_{50}$ (pre-IR_{225}) and post-IR $IRSL_{225}$ signals from 12 of the aliquots used for dating 14 of the samples in this study (i.e. 168 aliquots in total). For a subset of four samples (Tana 134/1, 5, 14, 15; $n = 48$), measurements were also made using the $IRSL_{50}$ signal alone to determine the fading rate for the $IRSL_{50}$ signal (rather than using an $IRSL_{50}$ (pre-$IRSL_{225}$) signal); it is the $IRSL_{50}$ fading rates from the measurements of the $IRSL_{50}$ signal alone that are presented in this paper.

Rates of anomalous fading are difficult to assess, even where measurements span a number of decades of time, as illustrated by the scatter in measured fading rates for both the post-IR $IRSL_{225}$ and $IRSL_{50}$ data from the polymineral fine-grain discs in this study (Fig. 4). Nevertheless, Fig. 4 demonstrates that there are clear differences in the rate of fading between the $IRSL_{50}$ and post-IR $IRSL_{225}$ signals; the mean fading rate for the $IRSL_{50}$ signal is 2.6 ± 1.3%/decade ($n = 47$, se $= 0.2$), compared to a lower mean value of 0.6 ± 1.1%/decade ($n = 168$, se $= 0.1$) for the post-IR $IRSL_{225}$ signal. This low fading rate for the post-IR $IRSL_{225}$ signal is comparable with fading rates measured for fast-component dominated quartz (e.g. Thiel et al., 2011; Buylaert et al., 2012), a mineral which is widely believed not to fade. Thiel et al. (2011), Buylaert et al. (2012, 2013) and Roberts (2012) all comment that low fading rates of less than 1–1.5% are difficult to assess and may in fact be an artefact of measurement. For this reason, the post-IR $IRSL_{225}$ ages presented in this study are not corrected for anomalous fading.

4.4. Luminescence ages

The post-IR $IRSL_{225}$ ages for the polymineral fine-grains prepared from 15 samples from Lake Tana, taken from the core between ~3 m and 90 m depth, are given in Table 2, and are shown plotted against depth in Fig. 5. The post-IR $IRSL_{225}$ ages span a range from ~4 ka to 256 ka, and show a progression down-section that is consistent with the stratigraphy when the uncertainties on each age are taken into account. Two samples, 134/9 and 134/13 (~29 and 55 m depth, respectively), have mid-point post-IR $IRSL_{225}$ ages which are younger than that of the overlying sample, but nevertheless they agree with the ages of the overlying samples within 2 sigma uncertainties (Table 2; Fig. 5). In spite of extensive consideration of the D_e and dose-rate components and the core characteristics at sample locations throughout the core, the cause of the reversal in the mid-point ages of samples 134/9 and 134/13 compared to the overlying samples is not known. However, it is interesting to note that these two samples are each located on the boundary of the two major changes in the seismic facies identified during the surveys of the lake sediments. The seismic survey data revealed a change at 53 m depth from an underlying basin-fill facies with horizontal planar reflectors ('Seismic Unit 1' of Lamb et al., 2018) to an overlying prograding wedge formation containing evidence of some erosion events ('Seismic Unit 2' of Lamb et al., 2018), which in turn changes to overlying sediments showing marked cyclicity in seismic facies from 33 m depth upwards ('Seismic Unit 3' of Lamb et al., 2018).

In seeking explanations for the reversal in the mid-point ages of samples 134/9 and 134/13 (i.e. disregarding uncertainties) compared to the samples that overlie them, differences in the efficacy of bleaching prior to deposition could be suggested. However, section 4.2 considered evidence to suggest that all samples were fully-bleached on deposition and hence this does not appear to be a viable explanation. Whilst sample 134/13 (55 m depth) does fall slightly away from the exponential fit to the $IRSL_{50}$ versus post-IR $IRSL_{225}$ data shown in Fig. 3, the data-point for sample 134/13 still lies within 10% of this fit and hence could be regarded as within acceptable limits given the coherence of the dataset as a whole (as discussed in section 4.2; Buylaert et al., 2013). This suggests that sample 134/13 is equally well-bleached as all the other samples in this study, including sample 134/9. However, even if sample 134/13 was not fully-bleached on deposition, contrary to the findings of section 4.2, it should be noted that incomplete bleaching would give rise to an older age for sample 134/13, whereas the mid-point ages observed for samples 134/9 and 134/13 are actually younger than the samples that overlie them (if errors are excluded). In spite of not managing to identify the reasons for reversal of the mid-points of samples 134/9 and 134/13, noted in Fig. 5 and outlined in the discussions above, it is important to remember that all 15 of the samples in this study are in chronostratigraphic order with overlying samples when the uncertainties on the ages are taken into account. In conclusion, as all of the post-IR $IRSL_{225}$ ages in this study agree with overlying ages within uncertainties, and pass all the quality control checks discussed, and there is no obviously discrepant data that can be identified by comparison of D_e or dose

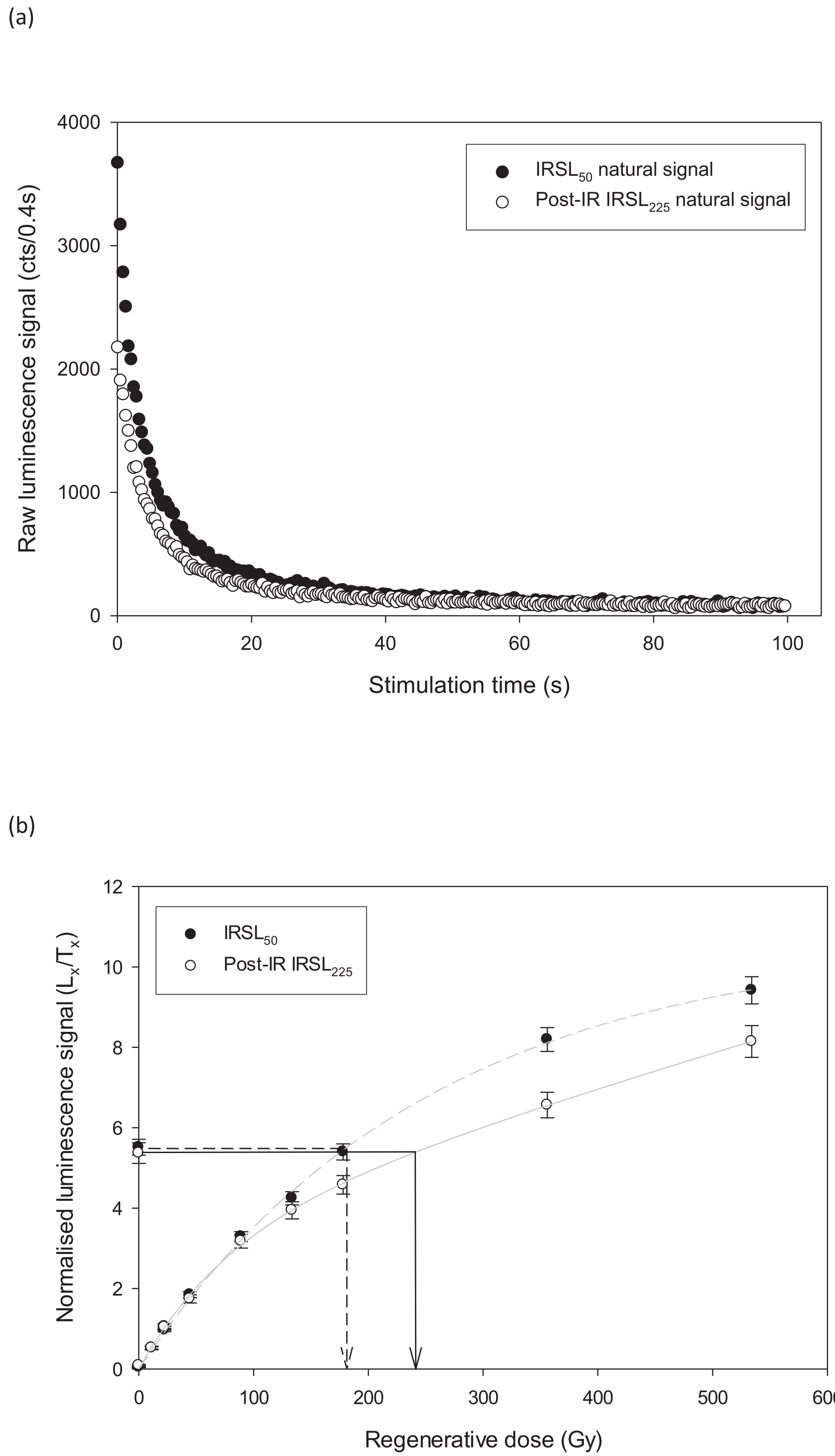

Fig. 2. Typical (a) decay curves and (b) dose response curves for $IRSL_{50}$ and post-IR IR_{225} signals from the same aliquot, Lake Tana sample 134/14.

rate data or through examination of the core, there is no objective reason to exclude any of the ages from further discussion or from use in the development of age models.

Applying a linear fit to the three uppermost post-IR IRSL ages (which are all Holocene in age), gives an R^2 value of 0.9997, and through extrapolation implies an age at the surface of the core of

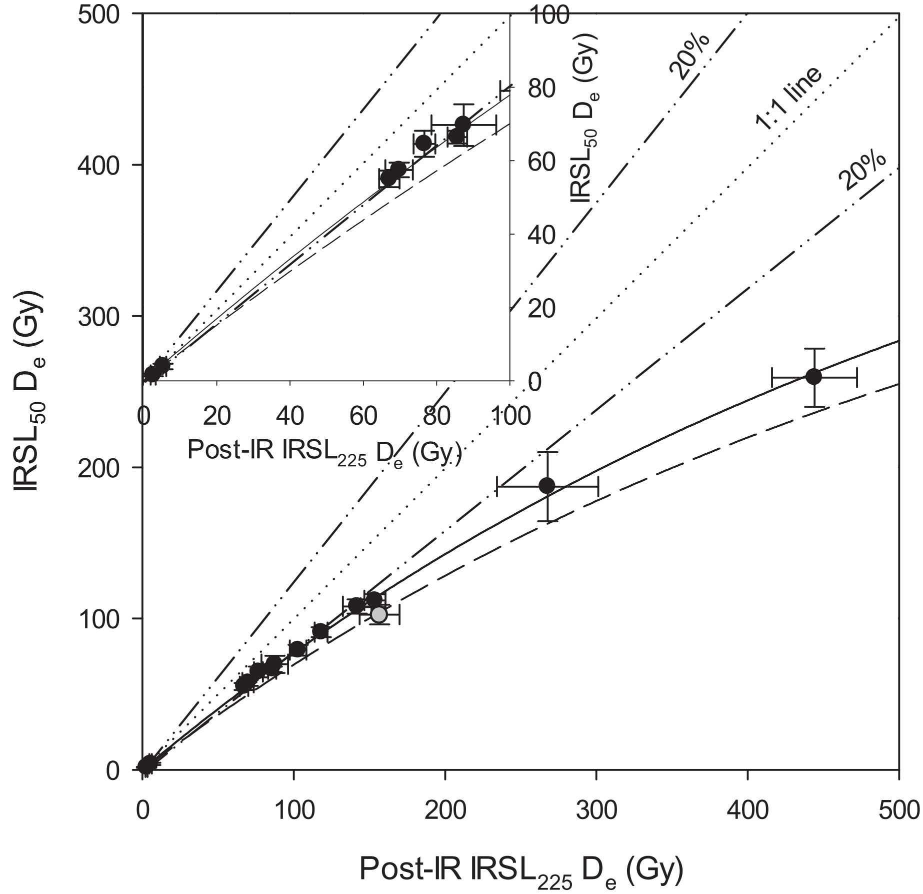

Fig. 3. Equivalent dose (D_e) values for samples 134/1 to 134/15, determined using $IRSL_{50}$ versus post-IR $IRSL_{225}$ signals measured from the same aliquots; the data-point shown in grey is sample 134/13, discussed in section 4.4. Each point shown is the mean of between 12 and 24 aliquots, and the error bars indicate the standard deviation. The solid line shows an exponential fit to the data, whilst the dashed line denotes 90% of this exponential fit; this relationship, proposed by Buylaert et al. (2013), is consistent with the behaviour expected from comparison of signals with different rates of anomalous fading. The dotted line indicates unity, and the dashed-dotted lines indicate ±20% of unity.

944 years. This might imply that an age offset of ~1 ka should apply to all of the ages throughout the study due to difficulty in resetting the post-IR $IRSL_{225}$ signal prior to deposition. Alternatively, it is likely that the upper sediments were not fully retrieved due to the difficulties of sampling suspended sediments in the uppermost sediment layers within the lake, which in turn would minimise any offset in the age calculated at the sediment surface due to there being a greater thickness of sediment in the upper unit than has been retrieved and accounted for in these calculations. In any case, even if the sediment accumulation rate in the late Holocene is the same as that determined from the early-to-mid Holocene (using the three uppermost ages which span 4.28–9.66 ka; Table 2), then from considering the projected uppermost age, and from examination of the IR_{50} and post-IR $IRSL_{225}$ signals compared in Fig. 3 (which implies that the sediments were well-bleached on deposition), it would seem that the maximum age offset in the post-IR $IRSL_{225}$ ages is likely to be ~1 ka, which obviously becomes of decreasing significance with increasing depth (and hence age) down-core. This ~1 ka maximum estimated age offset does not seem unreasonably low, given the relatively low levels to which the post-IR $IRSL_{225}$ signal from three Holocene samples was bleached within 4 only hours' exposure from the SOL2 solar simulator in the laboratory (1.3 ± 1.0 Gy).

4.5. Comparison of luminescence ages with independent chronology

For the upper part of the core, the post-IR $IRSL_{225}$ ages generated (Table 2) can be compared against independent chronology derived from radiocarbon dating (Table 3). Thirteen bulk sediment samples were taken from cores 07TL1 and PT07-2 for AMS radiocarbon dating at the NERC Radiocarbon Facility and AMS Laboratory, SUERC East Kilbride (Freeman et al., 2008), and prepared as outlined in Lamb et al. (2018); no terrestrial macrofossils were found. A sample-specific background was determined using deep sediments (i.e. beyond radiocarbon detection limits) from Lake Tana, giving a value of 0.54 ± 0.09% modern ^{14}C (n = 7), which is higher than the standard organic background material usually used for background determination, and was used to correct results. Of the thirteen samples taken for dating, eight returned finite values above the detection limit (Fig. 5; Table 3), and the remaining five samples, which also had low carbon contents (0.1–1.2% after sample pretreatment), were indistinguishable from background (Table 3). The four ^{14}C ages determined in the uppermost 14 m of the sediment core show an increase in age with depth, and are commensurate with the luminescence ages determined using the post-IR $IRSL_{225}$ signal (Fig. 5), suggesting that the luminescence ages generated in

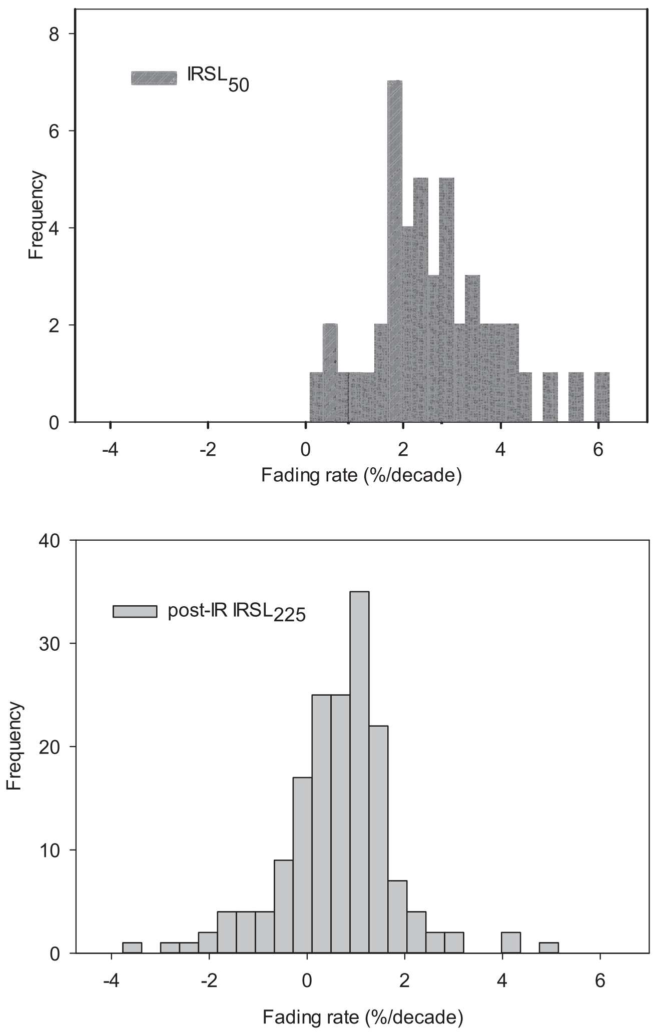

Fig. 4. Fading rates for the post-IR IR_{225} signal derived from 14 samples (lower figure; Tana 134/1–5 and 134/7–15; n = 168 data-points); the upper figure shows the fading rates determined for the IR_{50} signal alone (i.e. NOT using an $IRSL_{50}$ (pre-$IRSL_{225}$) signal) for a subset of four samples (Tana 134/1, 5, 14, 15; n = 47 data-points).

this study are appropriate. However, below ~30 m depth, there is little-to-no further progression of ^{14}C age with depth (Fig. 5), and the ages generated are approaching the detection limit for these samples (determined using the sample-specific background as ≥ 39,630 ^{14}C years B.P., Table 3). In contrast, the post-IR $IRSL_{225}$ ages continue to increase with increasing depth throughout the sediment core, extending well below the upper limit of radiocarbon to approximately 256 ka at 89 m depth (Fig. 5; Table 2).

4.6. Chronology of Lake Tana

The use of luminescence dating complements radiocarbon dating but spans a much wider dating range, allowing the objective examination of accumulation rates over time throughout the entire core from Lake Tana; additionally, the typically abundant nature of the material for luminescence dating allows ages to be generated at almost any point throughout the core thereby removing the need for extensive interpolation between or extrapolations beyond data-points. Higher resolution sampling took place in the upper 60 m of the core sediments (luminescence samples 134/1 to 134/14) where the core recovery was most complete; below 63 m the core recovery was poorer (section 3) and sample 134/15 at 89 m depth provided a basal date for the sediment core. Taken as a whole, the 15 post-IR $IRSL_{225}$ ages suggest that sediment deposition at Lake Tana has taken place over the last ~250,000 years. The average sediment accumulation rate over the last 256,000 years is 0.35 mm/a, a rate which is comparable with those from Lake Bosumtwi (W. Africa) and Lake Malawi (S.E. Africa) which have rates of ~0.4–0.5 mm/a (calculated using data of Scholz et al., 2007). Luminescence ages can also be used to calculate sediment accumulation rates for each of the three seismic facies described by Lamb et al. (2018), and outlined in section 4 of the present paper, giving values of 0.37, 0.76, and 0.25 mm/a for the unit <33 m, 33–53 m, and >53 m respectively (Fig. 5). Clearly far more complex statistical models can be applied to the data to look at even finer variations in accumulation rate in Lake Tana over the last ~250,000 years (e.g. the Bayesian age-depth model constructed and discussed for this dataset by Lamb et al. (2018)). However, even the crude changes in simple linear accumulation rate between the three seismic facies highlighted in the present paper would have been missed if only the extrapolated radiocarbon chronology had been available. The linear sediment accumulation rate calculated based on extrapolation of the uppermost 14 m of the radiocarbon chronology would have been 0.41 mm/a across the entire 92 m core. The age estimate of the basal sediments would also have been quite different using data extrapolated from ^{14}C ages alone, being 217 cal kyr BP at 89 m depth, a 15% age underestimate compared to the luminescence age of 256 ka. Whilst in this example the extrapolated age based solely on ^{14}C ages broadly agrees (within ± 2σ uncertainties) with the directly-dated luminescence age for the base of the core, at other sites excessive extrapolation could equally yield ages which were wholly inaccurate; without direct dating, e.g. using luminescence dating, the accuracy of such extrapolations cannot be known. This case study demonstrates that the use of both radiocarbon and luminescence dating techniques provides a valuable cross-check for each method, and highlights the extended chronology potentially available through the use of luminescence methods for dating long lacustrine sediment records.

5. Conclusions

The benefit of using multiple chronometers within a given study is well established (e.g. Shanahan et al., 2013; Brauer et al., 2014), but this paper emphasises the role that luminescence dating specifically can now play in developing long chronologies, even in lacustrine settings. In studies of African lakes in particular, chronology is vital for our understanding of past environments over the timescales of modern human evolution and dispersal, but continuous age estimates from direct dating have proved difficult to obtain over these timescales using other hitherto more conventional methods for dating lake sediments. The work shown in this paper on the long lacustrine records preserved at Lake Tana demonstrates that thanks to numerous methodological and technological advances, luminescence dating can generate ages spanning the last several hundred thousand years, generating ages throughout the sediment core rather than relying on opportunistic discovery of suitable and sufficient tephra or organic materials, for example.

At Lake Tana, post-IR $IRSL_{225}$ luminescence ages were generated across the full 90 m of sediment core using polymineral fine-grains of 4–11 μm diameter. Comparison of two different luminescence signals that bleach at different rates suggested that all of the samples in this study were equally well bleached on deposition. The luminescence ages were corroborated in the upper part of the core by agreement with radiocarbon ages, and reached an age of 256 ka for the lower part of the core at 89 m depth. Relying solely

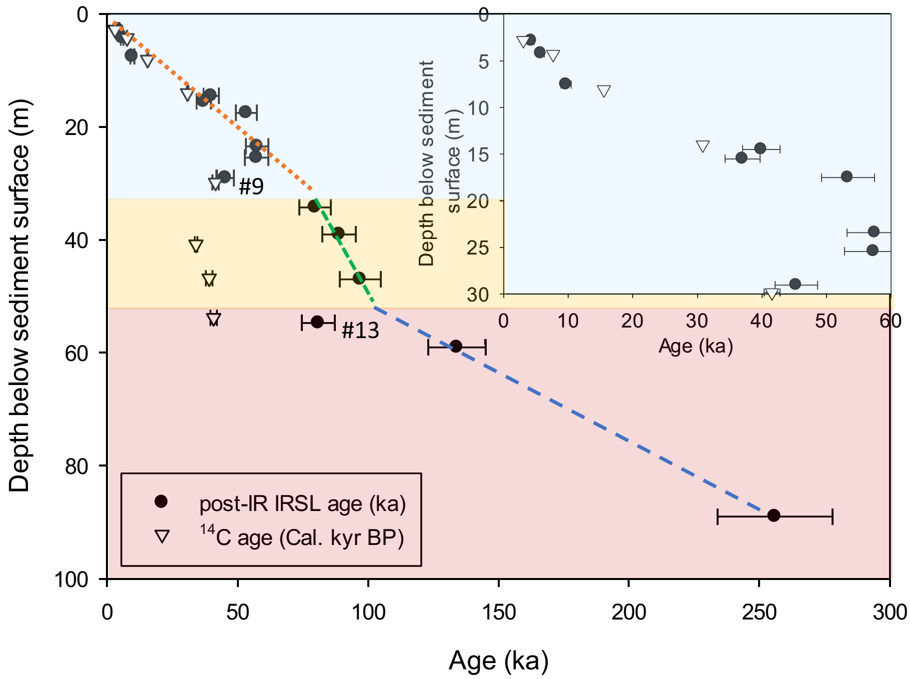

Fig. 5. Radiocarbon and post-IR IR_{225} luminescence ages plotted against depth below the sediment surface (m) for sediments from Lake Tana. Three different seismic facies have been identified within Lake Tana (discussed in Lamb et al., 2018), and are indicated here by different coloured shading. Luminescence samples number 9 and 13, mentioned in the text, are indicated by the labels '#9' and '#13' and lie just above the change in seismic facies in both cases. Inset shows the same data for the upper 30 m of sediment, for clarity. These radiocarbon and post-IR IR_{225} luminescence ages are also listed in Tables 3 and 2, respectively. The dotted and dashed lines indicate 3 different accumulation rates mentioned in section 4.6 (orange dotted = 0.37 mm/a; green short dash = 0.76 mm/a; blue long dash = 0.25 mm/a). (For interpretation of the references to colour in this figure legend, the reader is referred to the Web version of this article.)

Table 3
Radiocarbon (^{14}C) data obtained from analysis of bulk sediments from Lake Tana. See section 4.5 for discussion of these data.

Sample No.	SUERC Lab. code[a]	Stratigraphic depth (cm)	Delta^{13}C	% modern^{14}C	% modern^{14}C error	^{14}C Age (yr BP)	^{14}C Age error (yr BP)
07TL1/3/279 cm	SUERC-20086	279.0	−18.1	69.72	0.31	2898	35
07TL1/5/428 cm	SUERC-20087	428.0	−16.1	42.78	0.20	6821	38
07TL1/9/809 cm	SUERC-20090	809.0	−16.5	19.87	0.12	12980	47
PT07-2/4/1400 cm	SUERC-16457	1400.0	−20.0	3.63	0.09	26634	208
PT07-2/9/2985 cm	SUERC-16461	2985.0	−16.8	0.98	0.09	37154	739
PT07-2/13/4080 cm	SUERC-16462	4080.0	−17.6[b]	2.42	0.09	29901	301
PT07-2/15/4680 cm	SUERC-16463	4680.0	−18.1	1.36	0.09	34516	533
PT07-2/18/5380 cm	SUERC-16464	5380.0	−19.5[b]	1.09	0.09	36273	669
PT07-2/7/2237 cm	SUERC-16460	2237.0	−17.5	Indistinguishable from background, derived from deep sediments beyond the limit of $^{14}C = 0.54 \pm 0.09\%$ modern^{14}C [n = 7], equivalent to a detection limit of $0.54 + 2\sigma = 0.72\%$ modern^{14}C [≥ 39,630^{14}C years BP], as defined by Stuiver and Polach (1977)).			
PT07-2/20/5980 cm	SUERC-16465	5980.0	−20.9				
PT07-2/21/6280 cm	SUERC-16466	6280.0	−13.0				
PT07-2/28/8080 cm	SUERC-16470	8080.0	−16.0				
PT07-2/25/7180 cm	SUERC-16467	7180.0	−15.3				

[a] Scottish Universities Environmental Research Centre (SUERC) AMS Laboratory, East Kilbride, sample number.
[b] Denotes estimated delta^{13}C value as insufficient sample gas for an independent measurement.

on radiocarbon dating would have yielded, at best, a 15% age underestimation at the base of the Lake Tana core compared to the luminescence ages, and would have missed the opportunity to investigate the changes in accumulation rates through the sediment core; the lowermost radiocarbon ages could even have been misinterpreted as a rapid change in accumulation rate beyond ~14 m depth (~27 ka). Using luminescence ages in combination with radiocarbon dating revealed that sediment accumulation rates varied through the core from ~0.25 mm/a to more than triple this value, 0.76 mm/a. The Lake Tana sequence is one of the longest independently dated lacustrine sediment records in eastern Africa, demonstrating the significant contribution that luminescence dating can now make to development of chronologies for lacustrine sediments.

Acknowledgements

This work was undertaken as part of Natural Environment Research Council grant no. NE/DO12996/1, and with NERC Radiocarbon Facility support (NRCF010001 allocation number 1201.1006). The 2004 and 2006 seismic surveys were conducted by Richard Bates (University of St. Andrews) and D.G.H. (Bangor University), funded by NERC grant NER/B/S/2002/00540. Core retrieval was undertaken by. H.F.L., Sarah Davies, Mike Marshall, and Harry

Toland, (all Aberystwyth University), with scientific and logistical support from members of the Department of Earth Sciences at Addis Ababa University, especially the late Mohammed Umer; Addis Zeleke of Addis Geosystems plc; the Amhara Region Agricultural Research Institute. ICP measurements were conducted by J.N. Walsh (Royal Holloway University, London). Antony Smith (Aberystwyth University) is thanked for production of the location map, Fig. 1. Two anonymous reviewers are thanked for their helpful comments on the manuscript.

We are pleased to be able to contribute to this Special Issue of QSR, and delighted to do so with a paper that includes Henry Lamb as a co-author. HMR would like to thank Henry for "getting her into lakes", as it were, and for the various stimulating discussions, great personal connections, and fascinating opportunities that this collaborative research with Henry has brought. CLB would like to thank Henry for his collaborative ethos and support for NERC Radiocarbon Facility and as an enthusiastic member of the NRCF Steering Committee. DGH adds a personal commentary, the spirit of which will be shared by many colleagues who have worked with Henry over the years: "Henry has been a wonderful person to work with. Previously, I was primarily a marine engineering geophysicist, but his invitation to join him and the wider research team in various Ethiopian field studies opened up the whole field of tropical palaeoclimatology to me; he has provided so many opportunities of new fields of research, and with new colleagues. I will be forever grateful, not just for all this, but for being such a kind and kind-hearted person."

References

Abate, B., Koeberl, C., Buchanan, P.C., Körner, W., 1998. Petrography and geochemistry of basaltic and rhyodacitic rocks from Lake Tana and the Gimjabet-Kosober areas (North Central Ethiopia). J. Afr. Earth Sci. 26, 119–134.

Adamiec, G., Aitken, M., 1998. Dose-rate conversion factors: update. Ancient TL 16, 37–49.

Auclair, M., Lamothe, M., Huot, S., 2003. Measurement of anomalous fading for feldspar IRSL using SAR. Radiat. Meas. 37, 487–492.

Armitage, S.J., Bristow, C.S., Drake, N.A., 2015. West African monsoon dynamics inferred from abrupt fluctuations of Lake Mega-Chad. Proc. Natl. Acad. Sci. Unit. States Am. 112, 8543–8548.

Bates, C.R., Lamb, H.F., Umer, M., 2007. High-resolution seismic investigation of Lake Tana, northern Ethiopia. Near Surf. Geophys. 5, 243–250.

Burnett, A.P., Soreghan, M.J., Scholz, C.A., Brown, E.T., 2011. Tropical East African climate change and its relation to global climate: a record from Lake Tanganyika, Tropical East Africa, over the past 90+ kyr. Palaeogeogr. Palaeoclimatol. Palaeoecol. 303, 155–167.

Burrough, S.L., Thomas, D.S.G., 2008. Late Quaternary lake-level fluctuations in the Mababe Depression: middle Kalahari palaeolakes and the role of Zambezi inflows. Quat. Res. 69, 388–403.

Burrough, S.L., Thomas, D.S.G., 2009. Geomorphological contributions to palaeolimnology on the African continent. Geomorphology 103, 285–298.

Burrough, S.L., Thomas, D.S.G., Shaw, P.A., Bailey, R.M., 2007. Multiphase Quaternary highstands at Lake Ngami, Kalahari, northern Botswana. Palaeogeogr. Palaeoclimatol. Palaeoecol. 253, 280–299.

Buylaert, J.P., Murray, A.S., Thomsen, K.J., Jain, M., 2009. Testing the potential of an elevated temperature IRSL signal from K-feldspar. Radiat. Meas. 44, 560–565.

Buylaert, J.P., Jain, M., Murray, A.S., Thomsen, K.J., Thiel, C., Sohbati, R., 2012. A robust feldspar luminescence dating method for Middle and Late Pleistocene sediments. Boreas 41, 435–451.

Buylaert, J.P., Murray, A.S., Gebhardt, A.C., Sohbati, R., Ohlendorf, C., Thiel, C., Wastegård, S., Zolitschka, B., The PASADO Science Team, 2013. Luminescence dating of the PASADO core 5022-1D from Laguna Potrok Aike (Argentina) using IRSL signals from feldspar. Quat. Sci. Rev. 71, 70–80.

Brauer, A., Hajdas, I., Blockley, S.P.E., Ramsey, C.B., Christi, M., Ivy-Ochs, S., Moseley, G.E., Nowaczyk, N.N., Rasmussen, S.O., Roberts, H.M., Spotl, C., Staff, R.A., Svensson, A., 2014. The importance of independent chronology in integrating records of past climate change for the 60-8ka INTIMATE time interval. Quat. Sci. Rev. 106, 47–66.

Chapot, M.S., Roberts, H.M., Duller, G.A.T., Lai, Z.P., 2012. A comparison of natural- and laboratory-generated dose response curves for quartz optically stimulated luminescence signals from Chinese Loess. Radiat. Meas. 47, 1045–1052.

Chase, B.M., Meadows, M.E., 2007. Late Quaternary dynamics of southern Africa's winter rainfall zone. Earth Sci. Rev. 84, 103–138.

Cohen, A., Campisano, C., Arrowsmith, R., Asrat, A., Behrensmeyer, A., Deino, A., Feibel, C., Hill, A., Johnson, R., Kingston, J., Lamb, H., Lowenstein, T., Noren, A., Olago, D., Owen, R., Potts, R., Reed, K., Renaut, R., Schäbitz, F., Tiercelin, J., Trauth, M., Wynn, J., Ivory, S., Brady, K., O'Grady, R., Rodysill, J., Githiri, J., Russell, J., Foerster, V., Dommain, R., Rucina, S., Deocampo, D., Russell, J., Billingsley, A., Beck, C., Dorenbeck, G., Dullo, L., Feary, D., Garello, D., Gromig, R., Johnson, T., Junginger, A., Karanja, M., Kimburi, E., Mbuthia, A., McCartney, T., McNulty, E., Muiruri, V., Nambiro, E., Negash, E., Njagi, D., Wilson, J., Rabideaux, N., Raub, T., Sier, M., Smith, P., Urban, J., Warren, M., Yadeta, M., Yost, C., Zinaye, B., 2016. The Hominin Sites and Paleolakes Drilling Project: inferring the environmental context of human evolution from eastern African rift lake deposits. Sci. Drill. 21, 1–16.

Colarossi, D., Duller, G.A.T., Roberts, H.M., Tooth, S., Lyons, R., 2015. Comparison of paired quartz OSL and feldspar post-IR IRSL dose distributions in poorly bleached fluvial sediments from South Africa. Quat. Geochronol. 30, 233–238.

Davids, F., Roberts, H.M., Duller, G.A.T., 2010. Is X-ray core scanning non-destructive? Assessing the implications for optically stimulated luminescence (OSL) dating of sediment. J. Quat. Sci. 25, 348–353.

Divigalpitiya, W.M.R., 1982. Thermoluminescence Dating of Sediments. Unpublished M.Sc. thesis. Simon Fraser University, Burnaby.

Doran, P.T., Berger, G.W., Lyons, W.B., Wharton, R.A., Davisson, M.L., Southon, J., Dibb, J.E., 1999. Dating Quaternary lacustrine sediments in the McMurdo dry valleys, Antarctica. Palaeogeogr. Palaeoclimatol. Palaeoecol. 147, 223–239.

Duller, G.A.T., 2008. Single grain optical dating of Quaternary sediments: why aliquot size matters in luminescence dating. Boreas 37, 589–612.

Forman, S.L., Pierson, J., Gómez, J., 2007. Luminescence geochronology for sediments from Lake El'gygytgyn, northeast Siberia, Russia: constraining the timing of paleoenvironmental events for the past 200 ka. J. Paleolimnol. 37, 77–88.

Freeman, S.P.H.T., Dougans, A., McHargue, L., Wilcken, K.M., Xu, S., 2008. Performance of the new single stage accelerator mass spectrometer at the SUERC. Nucl. Instrum. Methods Phys. Res. B 226, 2225–2228.

Grün, R., 2009. The "AGE" program for the calculation of luminescence age estimates. Ancient TL 27, 45–46.

Guralnik, B., Jain, M., Herman, F., Ankjærgaard, C., Murray, A.S., Valla, P.G., Preusser, F., King, G.E., Chen, R., Lowick, S.E., Kook, M., 2015. OSL-thermochronometry of feldspar from the KTB borehole, Germany. Earth Planet Sci. Lett. 423, 232–243.

Huntley, D.J., Lamothe, M., 2001. Ubiquity of anomalous fading in K-feldspars and the measurement and correction for it in optical dating. Can. J. Earth Sci. 38, 1093–1106.

Juschus, O., Preusser, F., Melles, M., Radtke, U., 2007. Applying SAR-IRSL methodology for dating fine-grained sediments from Lake El'gygytgyn, north-eastern Siberia. Quat. Geochronol. 2, 187–194.

Kadereit, A., DeWitt, R., Johnson, T.C., 2012. Luminescence properties and optically (post-IR blue-light) stimulated luminescence dating of limnic sediments from northern Lake Malawi - chances and limitations. Quat. Geochronol. 10, 160–166.

Kars, R.H., Wallinga, J., Cohen, K.M., 2008. A new approach towards anomalous fading-correction for feldspar IRSL dating-tests on samples in field saturation. Radiat. Meas. 43, 786–790.

Kars, R.H., Wallinga, J., 2009. IRSL dating of K-feldspars: modelling natural dose response curves to deal with anomalous fading and trap competition. Radiat. Meas. 44, 594–599.

Kebede, S., Travia, Y., Alemayehub, T., Marc, V., 2006. Water balance of Lake Tana and its sensitivity to fluctuations in rainfall, Blue Nile basin, Ethiopia. J. Hydrol. 316, 233–247.

King, G., Burow, C., Roberts, H.M., Pearce, N., 2018. Age determination using feldspar: evaluating fading-correction model performance. Radiat. Meas. 119, 58–73.

Lamb, H.F., Bates, C.R., Coombes, P.M.V., Marshall, M.H., Umer, M., Davies, S.J., Dejen, E., 2007. Late Pleistocene desiccation of lake Tana, source of the Blue Nile. Quat. Sci. Rev. 26, 287–299.

Lamb, H.F., Bates, C.R., Bryant, C.L., Davies, S.J., Huws, D.G., Marshall, M.H., Roberts, H.M., 2018. 150,000-year palaeoclimate record from northern Ethiopia supports early, multiple dispersals of modern humans from Africa. Sci. Rep. 8, 1077.

Li, B., Jacobs, Z., Roberts, R.G., Li, S.H., 2014. Review and assessment of the potential of post-IR IRSL dating methods to circumvent the problem of anomalous fading in feldspar luminescence. Geochronometria 41, 178–201.

Long, H., Lai, Z., Wang, N., Zhang, J., 2011. A combined luminescence and radiocarbon dating study of Holocene lacustrine sediments from arid northern China. Quat. Geochronol. 6, 1–9.

Morthekai, P., Jain, M., Cunha, P.P., Azevedo, J.M., Singhvi, A.K., 2011. An attempt to correct for the fading in million year old basaltic rocks. Geochronometria 38, 223–230.

Moska, P., Poręba, G., Bluszcz, A., Wiszniowska, A., 2008. Combined IRSL/OSL dating on fine grains from Lake Baikal sediments. Geochronometria 31, 39–43.

Murray, A.S., Wintle, A.G., 2000. Luminescence dating of quartz using an improved single-aliquot regenerative-dose protocol. Radiat. Meas. 32, 57–73.

Murray, A.S., Olley, J.M., 2002. Precision and accuracy in the optically stimulated luminescence dating of sedimentary quartz: a status review. Geochronometria 21, 1–16.

Nicholson, S.E., 2017. Climate and climatic variability of rainfall over eastern Africa. Rev. Geophys. 55, 590–635.

Partridge, T.C., Demenocal, P.B., Lorentz, S.A., Paiker, M.J., Vogel, J.C., 1997. Orbital forcing of climate over South Africa: a 200 000-year rainfall record from the Pretoria Saltpan. Quat. Sci. Rev. 16, 1–9.

Prescott, J.R., Hutton, J.T., 1994. Cosmic ray contributions to dose rates for luminescence and ESR dating: large depths and long-term time variations. Radiat. Meas. 23, 497–500.

Rees-Jones, J., 1995. Optical dating of young sediments using fine-grain quartz. Ancient TL 13, 9–14.

Rittenour, T., 2008. Luminescence dating of fluvial deposits: applications to geomorphic, paleoseismic and archaeologic research. Boreas 37, 613–635.

Rhodes, E.J., 2011. Optically stimulated luminescence dating of sediments over the past 200,000 years. Annu. Rev. Earth Planet Sci. 39, 461–488.

Roberts, H.M., 2008. The development and application of luminescence dating to loess deposits: a perspective on the past, present and future. Boreas 37, 483–507.

Roberts, H.M., 2012. Testing Post-IR IRSL protocols for minimising fading in feldspars, using Alaskan loess with independent chronological control. Radiat. Meas. 47, 716–724.

Scholz, C.A., Johnson, T.C., Cohen, A.S., King, J.W., Peck, J.A., Overpeck, J.T., Talbot, M.R., Brown, E.T., Kalindekafe, L., Amoako, P.Y.O., Lyons, R.P., Shanahan, T.M., Castañeda, I.S., Heil, C.W., Forman, S.L., McHargue, L.R., Beuning, K.R., Gomez, J., Pierson, J., 2007. East African megadroughts between 135 and 75 thousand years ago and bearing on early-modern human origins. Proc. Natl. Acad. Sci. Unit. States Am. 104, 16416–16421.

Shanahan, T.M., Peck, J.A., McKay, N., Heil, C.W., King, J., Forman, S.L., Hoffmann, D.L., Richards, D.A., Overpeck, J.T., Scholz, C.A., 2013. Age models for long lacustrine sediment records using multiple dating approaches – an example from Lake Bosumtwi, Ghana. Quat. Geochronol. 15, 47–60.

Stuiver, M., Polach, H.A., 1977. Discussion: reporting of ^{14}C data. Radiocarbon 19, 355–363.

Thiel, C., Buylaert, J.P., Murray, A., Terhorst, B., Hofer, I., Tsukamoto, S., Frechen, M., 2011. Luminescence dating of the Stratzing loess profile (Austria) – testing the potential of an elevated temperature post-IR IRSL protocol. Quat. Int. 234, 23–31.

Thomsen, K.J., Murray, A.S., Jain, M., Bøtter-Jensen, L., 2008. Laboratory fading rates of various luminescence signals from feldspar-rich sediment extracts. Radiat. Meas. 43, 1474–1486.

Thomsen, K.J., Murray, A.S., Jain, M., 2011. Stability of IRSL signals from sedimentary K-feldspar samples. Geochronometria 38, 1–13.

Vandergoes, M., Newnham, R., Preusser, F., Hendy, C., Lowell, T., Fitzsimons, S., Hogg, A., Kasper, H.U., Schlüchter, Ch, 2005. Southern Ocean terrestrial record showing local modification of glacial–interglacial climate signals. Nature 436, 242–245.

Vijverberg, J., Sibbing, F.A., Dejen, E., 2009. Lake Tana: source of the Blue Nile. In: The Nile, Monographiae Biologicae, vol. 89, pp. 163–192. III.

Visocekas, R., Guérin, G., 2006. TL dating of feldspars using their far-red emission to deal with anomalous fading. Radiat. Meas. 41, 942–947.

Wintle, A.G., 1973. Anomalous fading of thermoluminescence in mineral samples. Nature 245, 143–144.